

EIC Detector R&D Progress Report: Fall 2014

Project Name: eRD4, DIRC-based PID for the EIC Central Detector

PIs: P. Nadel-Turonski*, T. Horn, C. Hyde, Y. Ilieva, J. Schwiening

Date: 12/31/2014

Past

What was planned?

The main goals for the period since the last R&D meeting were:

1. Commission the high-B test facility (end of FY13)
2. Carry out the first production high-B test run (FY14)
3. Test the new advanced lens at the GSI test beam (end of FY13)
4. Analyze the data from the test run (FY14)
5. Simulate the new lens in prototype used at the test beam using both drcprop and GEANT, both to evaluate the performance and in the future use it for benchmarking the EIC detector simulation.
6. Start integration of the DIRC GEANT simulation with the full EIC detector.

What was achieved?

All planned goals were achieved.

High-B sensor tests

Sensors: We finally received the two small-pore (3 and 5 micron) MCP-PMTs from Katod, making it possible to close that procurement. A further MCP-PMT was provided free of charge by Hamamatsu. It had some minor issues, but these should not be important for a test of the gain change in a magnetic field. Both the Katod and Hamamatsu PMTs require new holders that will be manufactured in the spring for future tests. The tests performed in the fall used Photek and Photonis tubes, which were lent to us for this purpose free of charge. The two Photek tubes were single-anode MCP-PMTs, while Photonis provided one single-anode MCP-PMT and two Planacon 64-channel MCP-PMTs with different pore sizes. The tests with the three single-anode MCP-PMTs have now been concluded, and the Photek tubes have been returned.

Tests: In addition to various bench tests, two tests were conducted with a cold magnet (at liquid helium temperature). The first one was a commissioning run at the very end of FY14, which first tested all components of the facility (including ramping the FROST magnet up to 5 T), and in the second week initial data were taken with single anode MCP-PMTs. The commissioning of the facility was very successful, and the initial data allowed us to optimize

the setup and run plan for the first production run. The former included an observation that most of the tube housings were magnetic to a level that produced a very significant torque even in 1-2 T fields (at the center of the solenoid there are no translational forces), which potentially could interfere with the angular measurements. And, of course, in a future detector torque also is something that would need to be addressed mechanically.

The second run was carried out before Thanksgiving. It also lasted two weeks, and saw the completion of a comprehensive set of tests with the single-anode MCP-PMTs from Photek and Photonis - all the way up to 5 T. Holders and readout for the Planacons were only ready just before the run, and one of the Planacons turned out not to be working, so data taking with the Planacons was postponed until the next run, planned for late spring. Data analysis is currently underway, and we hope to have the results from the fall run ready this spring. Both runs saw a broad participation, including K. Park who had been funded from the R&D funds earlier in 2014, as well as students from ODU and USC who were not formally supported by the project.

Appendix: Some pictures and additional details from the high-B tests are included in appendix B.

Prototyping and simulations

Test beam: The new, advanced, three-layer, second-generation lens with a high index of refraction (no air gaps) was manufactured this summer in Germany on cost (\$17k) and in time for the test beam at GSI. Greg Kalicy, the ODU postdoc funded by the R&D program was at GSI both for the preparations as well as the data taking during the test beam period. Despite some minor problems, both the two-layer and the new three-layer lens (developed for the EIC) were successfully tested. After the tests, Greg continued working on the data analysis, as well as simulations of the lens in the test beam environment. In the actual lens, a number of small improvements had been made compared with the original simulations carried out by the previous postdoc, Helena, and it was important to implement them correctly. In late December, Greg went to Germany, where he is staying for a month. During this time he will be working on the analysis of the test beam and the simulations together with our collaborators at GSI.

Simulations: The simulation effort this fall had several goals.

The first, which was requested by the committee, was to check the results obtained by Helena. This is being carried out using drcprop (ray-tracing) but with a different reconstruction algorithm, as well as a parallel GEANT4 simulation. A key difference is that the three-layer lens used in the simulation now exactly corresponds to the physical lens that was build for the prototype.

The second goal, mentioned above, is to do a similar simulation, but corresponding to the geometry used for the test beam setup, which would provide a direct comparison with experiment. Both of these goals are pursued in parallel and progressing at a good pace.

The third goal is to start the integration of the standalone GEANT4 simulation developed by Roman Dzhygadlo (who is also on the proposal), which is used for the GEANT part of the EIC DIRC simulations, into the EIC simulation framework. The first steps have already been

taken for integration into the JLab GEMC framework, and eventually this could be extended to FAIRroot or any other GEANT4 framework.

What was not achieved, why not, and what will be done to correct?

All the goals for the fall of 2014 were achieved. However, since the FY15 R&D funds were not paid out last fall, this required a lot of improvisation. For instance, JLab paid for the liquid helium for the high-B tests from operations funds, and ODU and USC found other means to temporarily cover salaries and travel. However, this allowed us to continue the R&D throughout the fall with minimal impact on the schedule.

Future

What is planned for the spring and beyond? How, if at all, is this planning different from the original plan?

For the simulations, we need to finalize the three goals stated above. The first two will be ready this spring. The third will be a more ongoing effort, iterated as the EIC detector(s) develop. The next steps in for the simulation will, as stated in the proposal, be to see if the lens design can be further optimized optically. If so, we would incorporate those lessons into the final lens prototype. If it turns out that the current lens is hard to improve on, the final prototype will focus on radiation hardness. The current lens is only intended to test the optical properties, but the follow-up lens will be made of a more radiation-hard materials (for instance substituting NLAK with PbF₂). Once the optics are fully optimize, we will in the final year focus on the optimization of the expansion volume to match the lens.

For the high-B tests we plan to continue the tests of the wide array of sensors we already have in the pipeline, with at least one two-week run planned every semester. Given the variety of the sensors (the MCP-PMTs mentioned above as well as some SiPMs), we believe that we will be able to pin down the critical parameters for future photosensors to be used for an EIC DIRC, as well as other subsystems for the EIC detector. We do, however, intend to start publishing partial results from the tests as early as this summer or next fall.

What are critical issues?

At the moment we are confident that we are on track, and will be able to bring the R&D program to a successful conclusion as outlined in the proposal.

Additional information:

Appendix B

The High-Magnetic-Field (High-B) Sensor Testing Facility at Jefferson Lab was installed and commissioned in summer of 2014. The facility provides for gain evaluation of small photomultipliers (PMT) in magnetic fields, B , up to 5 T. A first data-taking run took place in November of 2014.

The facility consists of a superconducting solenoid (FROST), a cylindrical non-magnetic dark test box, and electronics. Figure 1 shows the magnet and the dark box during the November-2014 run.

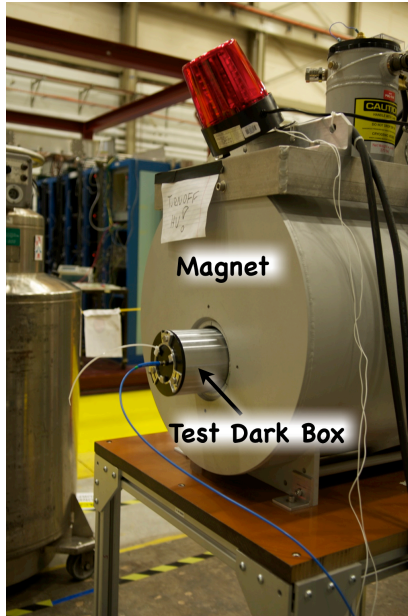


Figure 1 The setup of superconducting magnet and non-magnetic, dark test box during data taking. One can also see the optic fiber (blue cable) delivering light pulses to the box's interior.

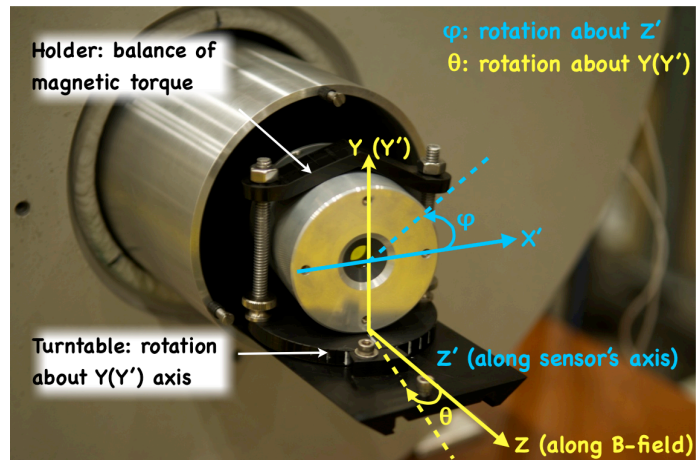


Figure 2 Mechanical setup inside of the test box, which holds the sensor in place and provides rotation capabilities. The sensor being tested rests on a turntable and is fixed in place by a custom-shaped holder. The turntable allows for rotations around the Y/Y' axis with a step of 5° . Additionally, sensors can be manually rotated around their own axis Z' (with a step size $\geq 5^\circ$ for cylindrically-shaped and a step size of 45° for rectangularly-shaped sensors). The sensor shown is Photech PMT210.

The magnet has a warm bore of 5-inch diameter and provides magnetic field of up to 5.1 T. In the center of the bore, the field inhomogeneity is $\leq 5 \times 10^{-5}$ over a cylindrical volume of a diameter of 1.5 cm and length of 5 cm. Given the small size of the sensors to be tested this feature ensures constancy of the B-field over the full length of the tested sensor. The test box is non-magnetic, has a cylindrical shape matching the diameter of the bore, and is 18 inches long. A plastic turntable that slides on a fixed rail holds the sensor and allows for a rotation about an axis perpendicular to the floor. Additionally, sensors can be rotated about their axis of symmetry. The turntable and the orientation capabilities of the setup are shown in Fig. 2.

The sensor tests are done by illuminating the photocathode with photons produced by a Light-Emitting Diode (LED). During the data taking in 2014, a 470-nm LED was used. To ensure illumination of the entire photo-cathode area, the light was diffused inside of the test box. The output signals of the photomultiplier were amplified by a factor of 200 in a pre-amplifier and fed into a flash Analog-to-Digital convertor, fADC250. The fADC samples the signal every 2 ns, thus digitizing the signal amplitude as a function of time. The total charge collected at the anode is obtained in a high-level analysis during the post-production data processing. The LED is controlled by a HP8116A pulse generator. During the tests the pulse generator was run at low intensity to simulate single-photoelectron mode of operation of the

tested PMT. The generator was also used to trigger the setup. A flow chart of the electronics is shown in Fig. 3.

The fADC was calibrated using a PS7120 charge generator. A preliminary analysis of the calibration data has yielded a conversion factor of 18.83 ± 0.39 fC/ADCch (see Fig. 4).

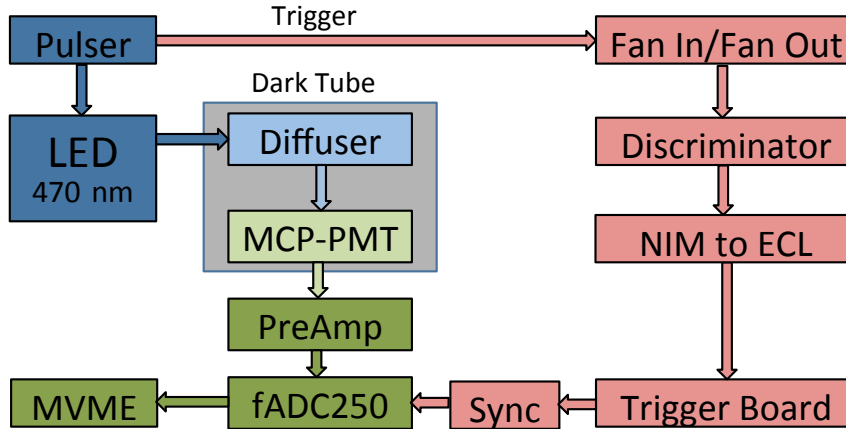


Figure 3 Schematic diagram of the electronics setup used to operate the PMT under test. The quantum efficiency for 470-nm photons of the sensors tested in 2014 was about 10 - 15%.

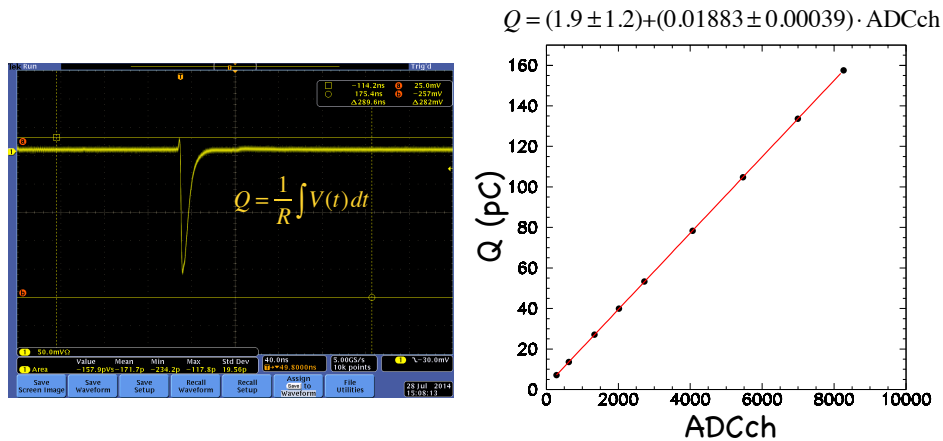


Figure 4 Left: The signal produced by the pulse generator was fed to a high-resolution digital oscilloscope. The signal was saved and analyzed in post-processing to obtain the total generated charge, Q . **Right:** The signals produced by the pulse generator were also fed to the fADC and analyzed in post-processing to obtain the total area of each pulse in ADC channel, ADCch. As expected the calibration is linear and yields 18.83 ± 0.39 fC/ADCch. The quoted uncertainty is very preliminary.

During Summer and Fall 2014 three single-anode Multichannel-Plate PMT (MCP PMT) were tested: Photek PMT210, Photek PMT240, and Photonis PP0365G (provided on loan by the manufacturers). Also, readout boards and voltage dividers for Planacons XP85112 and XP85012 were manufactured and tested

in the JLab Detector Lab under the supervision of Dr. C. Zorn. These will allow testing Planacon MCP PMTs in future runs. In addition the small-pore size MCP PMTs purchased under this R&D from Novosibirsk were received at JLab and are currently being equipped with a readout infrastructure for the upcoming measurement in Summer 2015.

Extensive data were collected for Photek PMT210 and Photonis PP0365G for various sets of (B, θ, φ) and operating high voltages. Due to its relatively large size, Photek PMT240 was evaluated for various B at only $\theta=0^\circ$ and $\varphi=0^\circ$. For systematic checks, a small sample of data was taken with a known Hamamatsu SiPM. While a detailed analysis of the collected data is undergoing, here we show some preliminary data from the first round of post-processing. To exemplify how the gain of the PMT changes with orientation and magnetic field, we show the pedestal-subtracted profile of the average signal, where the amplitudes of all recorded pulses at a given time are averaged over all the events for a given setting.

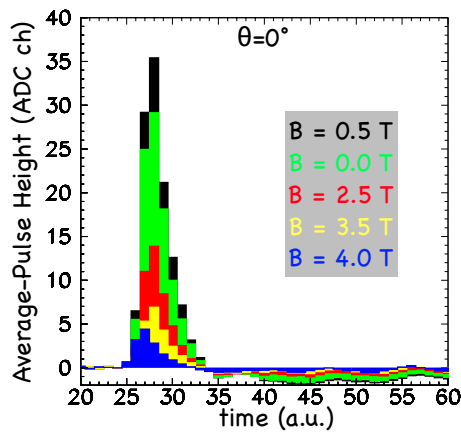


Figure 5 Time profile of the pedestal-subtracted average signal for various magnetic field strengths at $\theta=0^\circ$ and $\varphi=0^\circ$. The data are obtained with Photek PMT210.

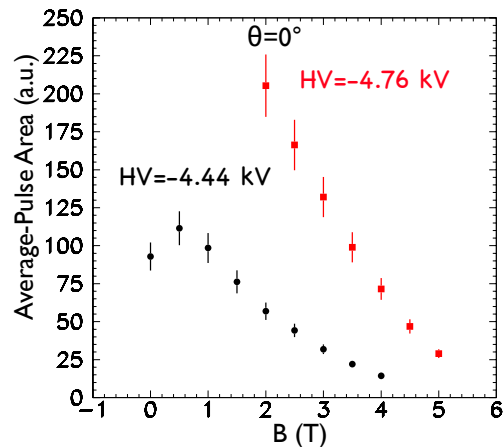


Figure 6 The area of the positive part of the pedestal-subtracted average signal for various field strengths and high voltages. The maximum high voltage for PMT210 is -4.8 kV.

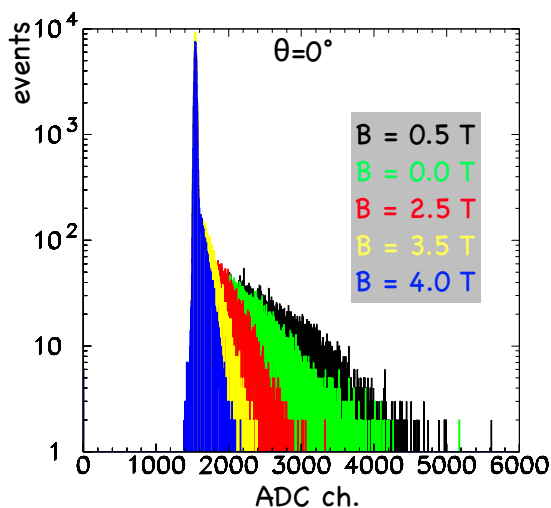
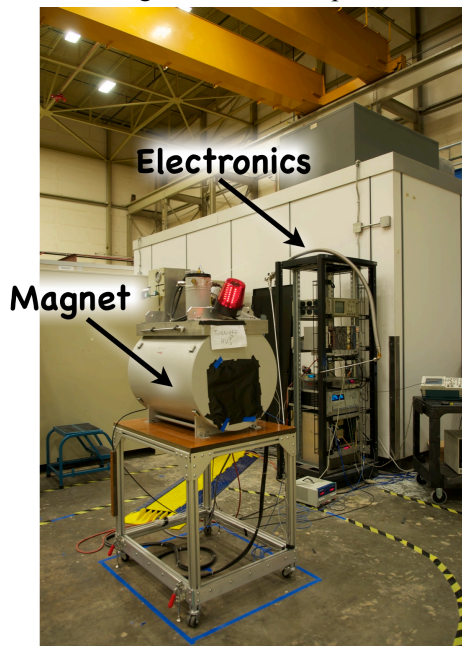


Figure 7 Event distribution of pulse area in units of ADCch for various field strengths. The large narrow peak at about 1530 ch is the pedestal. Data are collected from PMT210 at -4.4 kV.

Figure 5 shows how the average signal changes as the strength of the magnetic field increases for standard orientation of PMT210 ($\theta=0^\circ$ and $\varphi=0^\circ$, i.e. the photocathode is perpendicular to the direction of the field). Figure 6 shows the area of the positive part of the average signal as a function of B and high voltage for the same setting. The data suggest that the maximum gain of the MCP-PMT is reached at field strengths between 0.5 T and 1 T. Above 1 T, the gain smoothly decreases and no meaningful signal is observed above 4 T. Increasing the high voltage close to the maximum value, significantly increases the gain and allows to observe a clear signal up to 5 T. We would like to note that Fig. 5 and Fig. 6 show quantities that are proportional to the absolute charge collected on the anode, which includes single- and multi-

photoelectron events. The evaluation of the absolute gain of the MCP-PMT requires the identification of the single-photoelectron (1-phe) peak position relative to the pedestal on the event distribution over pulse area, where the pulse area is determined for each event in the sample. This distribution for various B at standard orientation of PMT210 is shown in Fig. 7. The distribution must be fitted to a complex function. For a good fit however, the 1-phe peak needs to be well pronounced and separated from the pedestal. While we do observe a good separation at the lowest fields, the spectra at higher fields cover much smaller range of amplitudes and non-pedestal events show as a tail to the pedestal. This means that we may not be able to evaluate the absolute gain of the sensor for each field. However, by evaluating the absolute gain at 0 T and determining the relative gain (relative to the gain at 0 T) at each setting from the total collected charge at that setting, we will be able to report the MCP-PMT gain as a function of setting (B , θ , φ). In addition to the data shown above, we scanned the PMT210 response from 0 T to 5 T at several θ between 0° and 30° as well as at $\theta=180^\circ$. For few θ , we did the field scans at $\varphi=0^\circ$, 90° , and 135° . Dark current measurements were done randomly for several settings. We collected similar extensive data set for PP0365G. The analysis of data is under way and we expect to have finalized results by March 2015. Studies of repeatability, making use of data at same setting randomly taken throughout the experiment, suggest that the uncertainty of our results is at least 10% (not including statistical and other systematic uncertainties). The stability of the pulser is most likely the major contributor to this uncertainty. As means to decrease this systematic uncertainty in future runs, we consider employing a reference PMT to the setup, which operates outside of the field. This would allow us to quantify changes in the light output of the LED and decrease the uncertainty of our results.

Additional figures of the setup



See also next page.

